molecules

MDPI

Article

Numerical Investigation of Graphene as a Back Surface Field Layer on the Performance of Cadmium Telluride Solar Cell

Devendra KC [1,†], Deb Kumar Shah [2,3,†], M. Shaheer Akhtar [3,4], Mira Park [5], Chong Yeal Kim [4], O-Bong Yang [2,3,4,*] and Bishweshwar Pant [5,*]

1 Electrical Department, Gabriel Elektro AS, 9700 Lakselv, Norway; devendrakc25@gmail.com
2 School of Semiconductor and Chemical Engineering, Jeonbuk National University, Jeonju 54896, Korea; dkshah149@gmail.com
3 Graduate School of Integrated Energy-AI, Jeonbuk National University, Jeonju 54896, Korea; shaheerakhtar@jbnu.ac.kr
4 New and Renewable Energy Materials Development Center (NewREC), Jeonbuk National University, Jeonbuk 56332, Korea; kimbo@jbnu.ac.kr
5 Carbon Composite Energy Nanomaterials Research Center, Woosuk University, Wanju, Chonbuk 55338, Korea; wonderfulmira@woosuk.ac.kr
* Correspondence: obyang@jbnu.ac.kr (O.-B.Y.); bisup@woosuk.ac.kr (B.P.)
† These authors are equally contributed to this work.

Abstract: This paper numerically explores the possibility of ultrathin layering and high efficiency of graphene as a back surface field (BSF) based on a CdTe solar cell by Personal computer one-dimensional (PC1D) simulation. CdTe solar cells have been characterized and studied by varying the carrier lifetime, doping concentration, thickness, and bandgap of the graphene layer. With simulation results, the highest short-circuit current (I_{sc} = 2.09 A), power conversion efficiency (η = 15%), and quantum efficiency (QE~85%) were achieved at a carrier lifetime of 1×10^3 μs and a doping concentration of 1×10^{17} cm^{-3} of graphene as a BSF layer-based CdTe solar cell. The thickness of the graphene BSF layer (1 μm) was proven the ultrathin, optimal, and obtainable for the fabrication of high-performance CdTe solar cells, confirming the suitability of graphene material as a BSF. This simulation confirmed that a CdTe solar cell with the proposed graphene as the BSF layer might be highly efficient with optimized parameters for fabrication.

Keywords: CdTe solar cell; graphene; back surface; efficiency; simulation

Citation: KC, D.; Shah, D.K.; Akhtar, M.S.; Park, M.; Kim, C.Y.; Yang, O-B.; Pant, B. Numerical Investigation of Graphene as a Back Surface Field Layer on the Performance of Cadmium Telluride Solar Cell. *Molecules* **2021**, *26*, 3275. https://doi.org/10.3390/molecules26113275

Academic Editor: Guanglin Xia

Received: 26 April 2021
Accepted: 26 May 2021
Published: 28 May 2021

1. Introduction

Modifications in the physical features of photovoltaic devices lead to improvement in the efficiency of a solar cell [1–3]. In CdTe/CdS solar cells, a metal layer with the work function ≥5.7 eV is needed to achieve a low contact resistance for proper functionality and sustainability. Generally, the Schottky barrier of a solar cell is rectified by a highly doped p-CdTe and insertion of a back surface field (BSF) layer at the CdTe/metal layer [4,5]. The BSF is an additional part, which consists of a heavily doped layer next to an absorber layer in the modern CdTe solar cell, i.e., a rear surface of the cell [6]. The highly doped BSF region acts as a barrier layer for minority mobile charge carriers at the CdTe/metal interface. The main purpose of providing a BSF layer in the structure of solar cells is to reduce the barrier width in the valence band and to reduce the recombination losses at the back surface of the CdS/CdTe solar cell [7–9]. The main technical problems of CdS/CdTe solar cells are related to higher efficiency, less material usage, and stable back contact formation [10,11]. These problems should be addressed and numerically evaluated to discover the unseen potentiality of CdS/CdTe solar cells for higher cell performance [10–13]. CdTe has good electronic properties, a high optical absorption coefficient of over 1×10^4/cm, and has a direct energy bandgap of 1.45 eV, which is very near to the optimal bandgap for solar cells [10,14]. However, a lower thickness of the absorber layer is required, which can help

to minimize cell material usage and reduce the cost of the manufacture of cells [10,15,16]. Due to the limitation of the reduction in the thickness of the absorber layer, the insertion of a thin back surface field (BSF) is essential to maintain a higher efficiency of CdTe solar cells [10,17]. The BSF layer of solar cells enhances the efficiency and FF because it degrades the shunting effects in the absorber layer [18]. A thickness of 1 μm for a BSF is sufficient for the recombination process of carriers at the interface of layers in the solar cells [7,19]. Providing a BSF layer in a CdTe solar cell may lead to some improvements like a thinner absorber layer with significant performance and reduction in cell fabrication cost [20]. The BSF layer helps the hole collection capability of CdTe cells due to the penetrating network and offers massive electrical transference routes to tie the individual graphene sheets [18,21,22]. Low-cost materials like graphene could be used as ultimate back contact without interrupting cell performance and stability.

The exploration of a stable and efficient back contact layer is important for the long-term stability of CdTe/CdS solar cells. CdTe has a high electron affinity and thus a high work function element is required to generate a good ohmic contact on p-type CdTe [10,23]. Graphene materials exhibit high carrier mobility (2×10^5 $cm^2/V{\cdot}s$) at room temperature, a high work function of 5.5 eV [18,24], excellent transparency (as they absorb light by ~2.3% across most of the ultraviolet (UV) and visible spectrum), marvelous thermal conductivity (~10^3 $W/m{\cdot}K$) [25], and a high melting point (~5000 K) [26]. Besides the atom-layer structure, they have a large surface area and graphene sheets have high flexibility. Therefore, low-cost graphene can be used in a wide range of applications, such as chemical sensors [27,28], medical devices [29], photodetectors [30], energy storage, [31], manufacturing roll-to-roll electronic devices [32], and solar cells [33,34]. Bhandari et al., in 2021, successfully incorporated added FeS_2-NC back contact in CdTe solar cells and showed good thermal stability under initial tests. Devices prepared with untreated FeS_2-NC back contacts display a strong "S-kink" behavior which correlates with a high hole-transport barrier arising from inter-NC organic surfactant molecules, but maximum efficiency was only 12.7% [7]. Liang et al., in 2012, successfully combined Cu nanowire-doped graphene (Cu NWs/graphene) as the back contact layer in thin-film CdTe solar cells. The efficiency of solar cells with Cu NWs/graphene was up to 12.1% [18]. The drawback with the Cu-based back contact layer is the Cu diffusion with the grain boundaries as well as across the junction.

In this work, a CdTe solar cell was designed and simulated using the PC1D simulation tool to investigate the influence of carrier lifetime, doping concentration, bandgap, and thickness of the BSF layer on the conversion efficiency of the CdTe solar cell. The carrier lifetime, doping concentration, and thickness of the BSF layer are critical parameters for the PV properties of solar cells. This modeling study aimed to check the effect of carrier lifetime, doping concentration, and thickness of BSF layer on the I_{sc}, V_{oc}, and efficiency and recommend the best possible combination for fabrication.

2. Materials and Methods

2.1. Solar Cell Structure and BSF Layer

The purpose of numerical investigation in the PV cell analysis is to examine the validity of the projected device structure's arranged cell geometry and cell efficiency. In this proposed model, p-type CdTe and n-type CdS were used as an absorber layer and window layer, respectively. An additional layer of highly doped graphene [35] was applied as a back surface field (BSF) layer next to the absorber layer on the substrate, as shown in Figure 1.

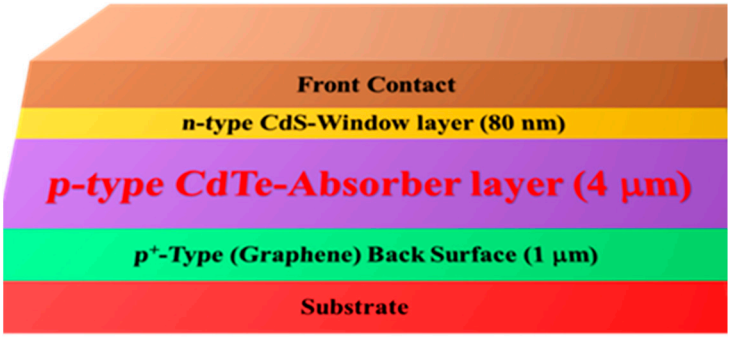

Figure 1. The device structure of graphene back surface-based CdTe solar cell.

The layers in this solar cell were organized according to the energy bandgap, in which the layer with a lower bandgap was placed on the bottom, while the layer with a higher bandgap was placed on the top surface [36]. The layer with a higher bandgap can absorb a wide range of solar radiation of a shorter wavelength [37]. An additional ultrathin layer of graphene as a BSF was added to reduce the recombination losses at the back contact, which enhances the efficiency of a solar cell.

2.2. PC1D Modeling Tool

The personal computer one-dimensional (PC1D) modeling tool is used to study the photovoltaic properties of solar cells, and it was developed by a team of the UNSW [38]. PC1D allows the simulation of the optoelectrical properties of semiconductor devices. The main advantages of PC1D include rapid calculation speeds, an intuitive user interface, and an extensive list of material and physical parameters. By varying the wavelength of the excitation light source, PC1D can calculate both current-voltage characteristics and the spectral quantum efficiency of a solar cell [39,40]. The PC1D software contains plentiful library files including numerous parameters for semiconductor devices such as GaAs, Ge, c-Si, GIN, CIGS, a-Si, AlGaAs, and InP [41–43]. In the simulation tool, the input key parameters, such as device area, device thickness, carrier concentration, bandgap, temperature, reflectance, etc., were used to elucidate the photovoltaic parameters of the solar cell. The detailed input parameters of this software have been summarized in Table 1. All simulations were executed under a constant light intensity of 0.1 W/cm^2 (AM) 1.5 at 300 K temperature. For all PV simulations, the bulk recombination time was set from 1 to 100 μs and the doping concentration in the solar cell was set in the range of 1×10^{15} to 1×10^{20} cm^{-3} as reported in previous research articles [44–46].

Table 1. Internal parameters of the PC1D simulation tool.

Parameters	CdS	CdTe	Graphene
Thickness	80 nm [7]	4 μm [7]	1 μm
Energy band gap (eV)	2.4 [47]	1.5 [47]	0.5 [48]
Electron affinity	4.2 [49]	4.28 [49]	4.7 [48]
Bulk recombination	1000 μs	1000 μs	10–10^6 μs
Doping concentration	1×10^{17} cm^{-3}	1×10^{16} cm^{-3}	1×10^{15}–1×10^{20} cm^{-3}
Excitation mode	Transient	Transient	Transient
Constant intensity	One sun	One sun	One sun
Dielectric constant	10	9.4	7.1
Temperature	300 K	300 K	300 K
Constant intensity	0.1 W/cm^{-2}	0.1 W/cm^{-2}	0.1 W/cm^{-2}
Primary light source	AM 1.5 D spectrum	AM 1.5 D spectrum	AM 1.5 D spectrum
Other parameters	Internal PC1D	Internal PC1D	Internal PC1D

3. Results and Discussion

3.1. Impact of Carrier Lifetime in BSF Layer

Carrier lifetime in the BSF layer has a very vital role in the efficiency of a solar cell. The probability of carriers reaching their respective direction's end before their recombination is higher when the carrier lifetime is longer [50]. The photovoltaic properties, like I_{sc}, V_{oc}, efficiency, and FF, were characterized in the range from 1 to 10^6 µs of carrier lifetime of the solar cells. When the carrier lifetime in the BSF layer increased from 1 to 10^3 µs, the PV properties of solar cells increased and, after that, these factors were saturated, increasing even further. The maximum values of I_{sc} = 2.09 A, V_{oc} = 0.809 V, η = 15% and FF = 88.54% were be observed at 1 × 10^3 µs of carrier lifetime, as shown in Figure 2a,b. Thus, the optimized value of carrier lifetime is 1 × 10^3 µs in the BSF layer of the CdTe solar cell.

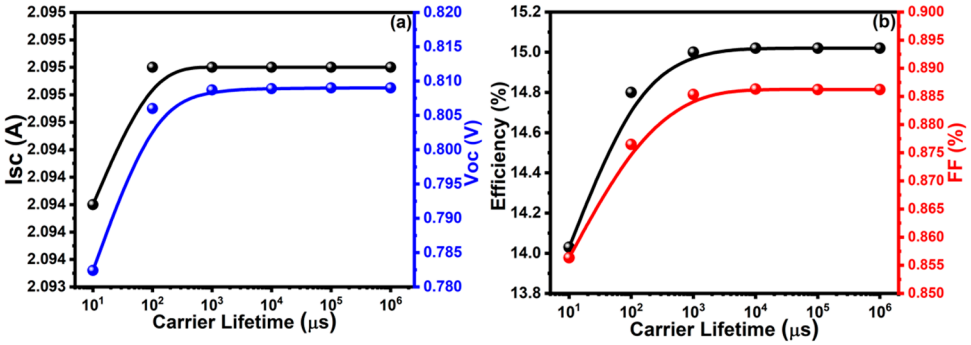

Figure 2. Analysis of (**a**) Isc and Voc, (**b**) efficiency and FF with carrier lifetime of BSF layer.

3.2. Impact of Doping Concentration in BSF Layer

A doping concentration is one of the decisive factors affecting the overall performance of the solar cell. The values of PV parameters such as I_{sc}, V_{oc}, efficiency, and FF increase with higher doping concentrations in the BSF layer due to an increase in band-bending in CdTe solar cells [51]. It is also proven that a very high doping concentration in the back contact layer can support the generation of a tunneling contact. It is known to be highly difficult to obtain high p-type doping in CdTe material due to self-compensation [52]. The PV properties (I_{sc}, V_{oc}, η, and FF) were characterized in the range from 1 × 10^{15} to 1 × 10^{20} cm^{-3} of doping concentration in the BSF layer of the solar cell. When the doping concentration in the BSF layer increased from 10^{15} to 10^{17} cm^{-3}, the PV properties remained unchanged and, after that, started to decrease sharply with a further increase. Lower doping density leads to a wider depletion region, which is beneficial for the carrier collection and recombination process [53]. The optimum values of I_{sc} = 2.09 A, V_{oc} = 0.809 V, η = 15%, and FF = 88.55% were observed at 1 × 10^{17} cm^{-3} of doping concentration, as shown in Figure 3a,b. Thus, the optimized value of doping concentration is 1 × 10^{17} cm^{-3} in the BSF layer of the CdTe solar cell.

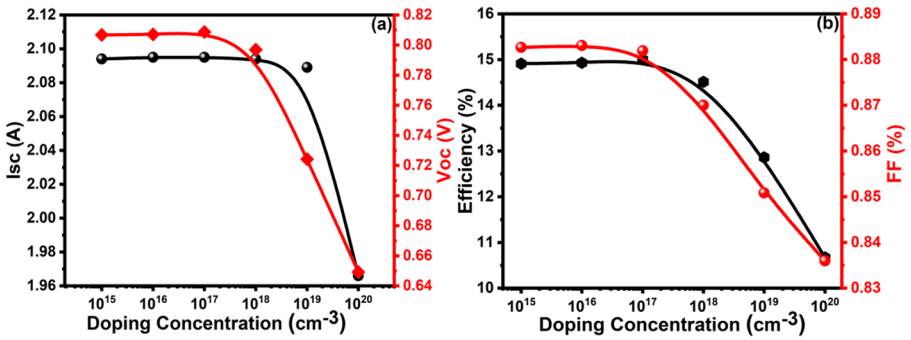

Figure 3. Analysis of (**a**) Isc and Voc, (**b**) efficiency and FF with a doping concentration of BSF layer.

3.3. Impact of the Thickness of BSF Layer

It is essential to control the optimal thickness of the BSF layer since an excessive thickness can cause fast degradation due to diffusion; however, a much thinner BSF layer gives insufficient intermixing and doping in the bulk CdTe [54]. The thickness of the BSF layer should be ultrathin, which is very difficult to control. The PV properties, such as I_{sc}, V_{oc}, η, and FF, were characterized in the range from 0.1 to 1.5 μm of the thickness of graphene as the BSF layer of the solar cell. The value of Isc increased with an increase in the thickness of the BSF layer, whereas the value of Voc decreased, as shown in Figure 4a. Similarly, the efficiency of a cell was increased with the increase in the thickness of the BSF layer, whereas the FF value was decreased, as shown in Figure 4b, so it is difficult to set the optimum thickness of the BSF layer. For efficient and practicable solar cell fabrication, an obtainable (i.e., possible) thickness of graphene as the BSF layer should be chosen. The optimum values of I_{sc} = 2.09 A, V_{oc} = 0.808 V, η = 15%, and FF = 88.53% were observed at 1 μm thickness of the BSF layer. Therefore, the optimum value of the thickness of graphene as the BSF layer might be 1 μm for fabrication.

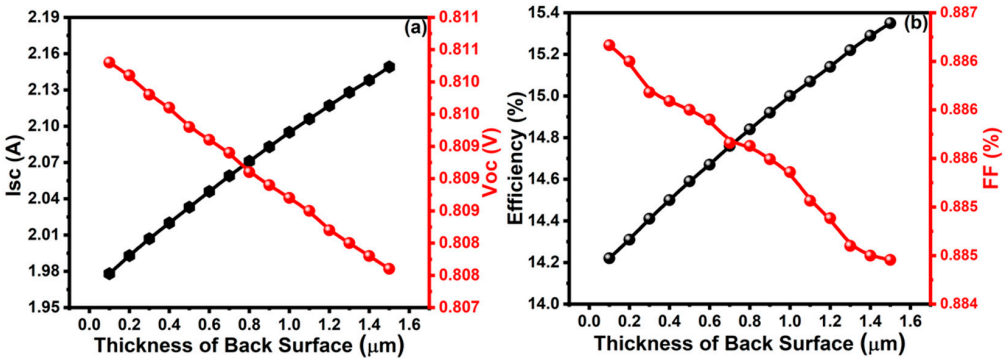

Figure 4. Analysis of (**a**) Isc and Voc, (**b**) efficiency and FF with the thickness of BSF layer.

3.4. Impact of Photogeneration Rate of Carriers in BSF Layer

Minority carrier transport parameters critically affect the function and performance of various p-n junction semiconductor devices with bipolar transistors and solar cells [55]. Various recombination processes were applied to find the carrier lifetime and diffusion length of the minority charge carriers in the emitter and all parts of the solar cell [56]. The thickness of the p-n junction was about 4 μm and the photogeneration rate was 1.22×10^{19} s^{-1} at that thickness, which is appropriate for recombination of charge carriers. The simulation result showed that the photogeneration rate increases logarithmically as the distance from the front increases, as shown in Figure 5, which might be suitable for efficient solar cells.

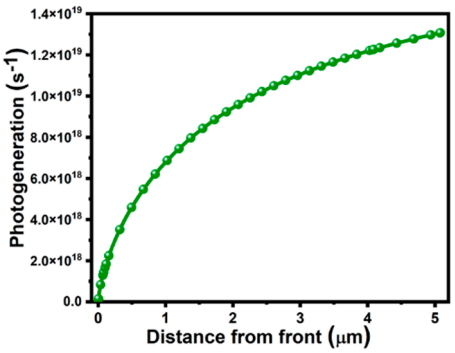

Figure 5. Analysis of cumulative photogeneration rate with distance from front in BSF layer.

3.5. Energy Bandgap of Layers in Solar Cell

The energy bandgap is the threshold energy that is required to excite electrons up to a state in the conduction band where they can participate in conduction [57]. The theoretical values of the energy bandgap are 2.42 eV [58], 1.45 eV [59], and 0.264–0.786 eV [60] for window (CdS), absorber (CdTe), and BSF (graphene) layers, respectively, at room temperature. When light radiation with a wide range of wavelengths enters the solar cell, it must cross through different materials with various energy bandgaps. The simulated values of energy bandgaps were 2.41, 1.5, and 0.5 eV for window (CdS), absorber (CdTe), and BSF (graphene) layers, respectively, as shown in Figure 6, which almost match the theoretical values. From the simulation, it was confirmed that the proposed solar cell structure is appropriate for fabrication.

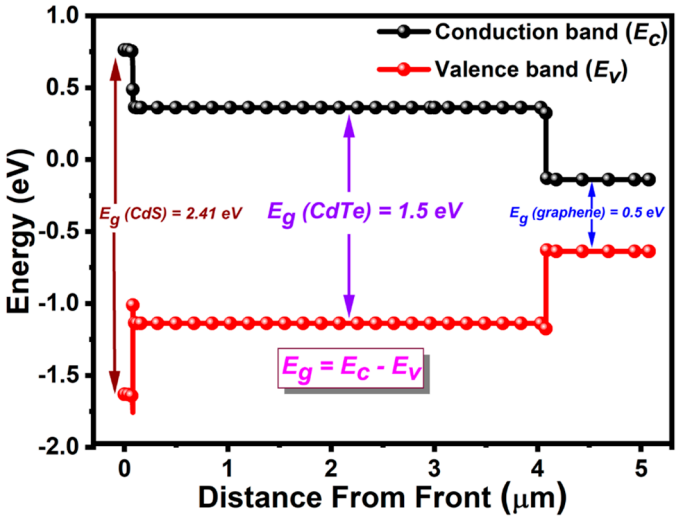

Figure 6. Analysis of bandgap energy of graphene BSF layer-based CdTe solar cell.

3.6. Photovoltaic Characteristics

The ultimate characteristic is the current, power, and efficiency curve to examine the overall efficiency of the solar cell. The simulation results exhibited the highest values of I_{sc} = 2.09 A, V_{oc} = 0.808 V, I_{mp} = 2.049 A, V_{mp} = 0.729 V, P_{max} = 1.5 W, and η = 15%, as shown in Figure 7. Quantum efficiency is also one of the most important characteristics to estimate the performance of the solar cell in the specific range of the wavelength. The internal quantum efficiency (IQE) was above 100% whilst an external quantum efficiency of approximately 85% was achieved in the wavelength range of 300–1000 nm, as shown in Figure 8.

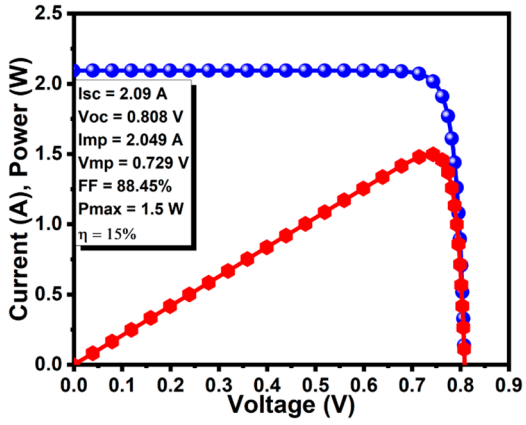

Figure 7. Analysis of current and power curve of graphene BSF layer-based CdTe solar cell.

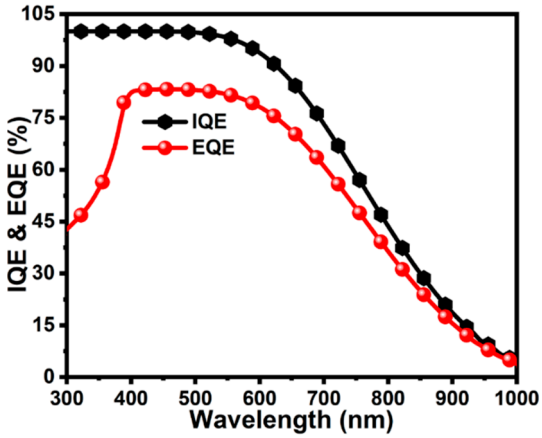

Figure 8. Analysis of quantum efficiency of graphene BSF layer-based CdTe solar cell.

The comparative study of the reported graphene back contact surface layer-based CdTe solar cells is listed in Table 2. This simulation presented impressive results and confirmed that the proposed structure of the solar cell could be suitable for efficient fabrication.

Table 2. Comparative study of the performance of graphene as BSF material-based CdTe solar cell.

BSF Materials	J_{sc} [mA/cm^2]	V_{oc} [V]	FF [%]	Efficiency [%]	References
Cu NWs/graphene	22.4	0.801	67.40	12.1	[61]
CuPs/graphene	21.3	0.805	68.10	11.7	[61]
Graphene	22.2	0.633	43.01	12.2	[62]
Graphene	40.0	0.511	65.03	13.2	[63]
Graphene	20.9	0.808	88.45	15	This work

4. Conclusions

The possibility of ultrathin layering and high efficiency of graphene material as a back surface field (BSF)-based CdTe solar cell has been simulated successfully using the PC1D simulation tool. The highest I_{sc} = 2.09 A, η = 15% and QE~85% by CdTe solar cell were accomplished when the graphene as a BSF layer had a carrier lifetime of 1×10^3 μs and doping concentration of 1×10^{17} cm^{-3}. The obtained results suggest that the thickness of the BSF graphene layer (1 μm) is ultrathin which is an appropriate and optimal thickness for the fabrication of high-performance CdTe solar cells. Therefore, the simulation results prove that the graphene as the BSF layer with ultrathin could be highly efficient, low cost, and providing the ease of fabrication for CdTe solar cells with excellent photovoltaic properties.

Author Contributions: D.K.C., methodology, investigation; D.K.S., software, validation, writing-original draft preparation; M.S.A., formal analysis, resources, review, and editing; B.P., data curation, correction in the original draft, visualization; M.P., data curation; C.Y.K., supervision, funding acquisition; O.-B.Y., project administration, supervision. All authors have read and agreed to the published version of the manuscript.

Funding: This research was funded by the Human Resources Program in Energy Technology of the Institute of Energy Technology Evaluation and Planning (KETEP) and granted financial resources from the Ministry of Trade, Industry & Energy, Republic of Korea (Project No.: 20204010600470).

Conflicts of Interest: The authors declare no conflict of interest.

References

1. Kazmi, S.A.A.; Khan, A.D.; Khan, A.D.; Rauf, A.; Farooq, W.; Noman, M.; Ali, H. Efficient materials for thin-film CdTe solar cell based on back surface field and distributed Bragg reflector. *Appl. Phys. A* **2019**, *126*, 46. [CrossRef]
2. Yuriy, N.L.; Alexander, N.S.; Vasiliy, A.T.; Dmitry, Y.P.; Svetlana, M.P.; Petr, V.D.; Sergei, N.C.; Sergey, A.P. Effect of core modification in star-shaped donor-acceptor oligomers on physical properties and photovoltaic performance. In Proceedings of the SPIE 10363, San Diego, CA, USA, 25 August 2017.
3. Shah, D.K.; Son, Y.-H.; Lee, H.-R.; Akhtar, M.S.; Kim, C.Y.; Yang, O.-B. A stable gel electrolyte based on poly butyl acrylate (PBA)-co-poly acrylonitrile (PAN) for solid-state dye-sensitized solar cells. *Chem. Phys. Lett.* **2020**, *754*, 137756. [CrossRef]
4. Hossain, M.S.; Amin, N.; Razykov, T.M. Prospects of Back Contacts with Back Surface Fields in High Efficiency Znxcd1-Xs /Cdte Solar Cells from Numerical Modeling. *Chalcogenide Lett.* **2011**, *8*, 187–198.
5. Amin, N.; Matin, M.A.; Aliyu, M.M.; Alghoul, M.A.; Karim, M.R.; Sopian, K. Prospects of Back Surface Field Effect in Ultra-Thin High-Efficiency CdS/CdTe Solar Cells from Numerical Modeling. *Int. J. Photoenergy* **2010**, *2010*, 1–8. [CrossRef]
6. Doroody, C.; Rahman, K.S.; Rosly, H.N.; Harif, M.N.; Haque, F.; Tiong, S.K.; Amin, N. Impact of high resistivity trans-parent (HRT) layer in cadmium telluride solar cells from numerical simulation. *J. Renew. Sustain. Energy* **2020**, *12*, 023702. [CrossRef]
7. Bhandari, K.P.; Koirala, P.; Paudel, N.R.; Khanal, R.R.; Phillips, A.B.; Yan, Y.; Collins, R.W.; Heben, M.J.; Ellingson, R.J. Iron pyrite nanocrystal film serves as a copper-free back contact for polycrystalline CdTe thin film solar cells. *Sol. Energy Mater. Sol. Cells* **2015**, *140*, 108–114. [CrossRef]
8. Demtsu, S.; Sites, J. Effect of back-contact barrier on thin-film CdTe solar cells. *Thin Solid Films* **2006**, *510*, 320–324. [CrossRef]
9. Shah, D.K.; Han, S.Y.; Akhtar, S.M.; Yang, O.-B.; Kim, C.Y. Effect of Ag Doping in Double Antireflection Layer on Crystalline Silicon Solar Cells. *Nanosci. Nanotechnol. Lett.* **2019**, *11*, 159–167. [CrossRef]
10. Matin, M.A.; Dey, M. High performance ultra-thin CdTe solar cell with Lead Telluride BSF. In Proceedings of the International Conference on Informatics, Electronics & Vision (ICIEV), Dhaka, Bangladesh, 23–24 May 2014; pp. 1–5.
11. Fang, Z.; Wang, X.C.; Wu, H.C.; Zhao, C.Z. Achievements and Challenges of CdS/CdTe Solar Cells. *Int. J. Photoenergy* **2011**, *2011*, 1–8. [CrossRef]
12. Wu, X. High-efficiency polycrystalline CdTe thin-film solar cells. *Sol. Energy* **2004**, *77*, 803–814. [CrossRef]
13. Shah, D.K.; Choi, J.; Devendra, K.C.; Akhtar, M.S.; Kim, C.Y.; Yang, O.B. Refined optoelectronic properties of silicon nanowires for improving photovoltaic properties of crystalline solar cells: A simulation study. *J. Mater. Sci. Mater. Electron.* **2021**, *32*, 2784–2795. [CrossRef]
14. Boudour, S.; Bouchama, I.; Bouarissa, N.; Hadjab, M. A study of CdTe solar cells using Ga-doped MgxZn1-xO buffer/TCO layers: Simulation and performance analysis. *J. Sci. Adv. Mater. Dev.* **2019**, *4*, 111–115. [CrossRef]
15. Bai, Z.; Yang, J.; Wang, D. Thin film CdTe solar cells with an absorber layer thickness in micro- and sub-micrometer scale. *Appl. Phys. Lett.* **2011**, *99*, 143502. [CrossRef]
16. Li, J.; Chen, X.; Yi, Z.; Yang, H.; Tang, Y.; Yi, Y.; Yao, W.; Wang, J.; Yi, Y. Broadband solar energy absorber based on monolayer molybdenum disulfide using tungsten elliptical arrays. *Mater. Today Energy* **2020**, *16*, 100390. [CrossRef]
17. Wilson, G.M.; Al-Jassim, M.; Metzger, W.K.; Glunz, S.W.; Verlinden, P.; Xiong, G.; Mansfield, L.M.; Stanbery, B.J.; Zhu, K.; Yan, Y.; et al. The 2020 photovoltaic technologies roadmap. *J. Phys. D Appl. Phys.* **2020**, *53*, 493001. [CrossRef]
18. Liang, J.; Bi, H.; Wan, D.; Huang, F. Novel Cu Nanowires/Graphene as the Back Contact for CdTe Solar Cells. *Adv. Funct. Mater.* **2012**, *22*, 1267–1271. [CrossRef]
19. Nakane, A.; Tampo, H.; Tamakoshi, M.; Fujimoto, S.; Kim, K.M.; Kim, S.; Shibata, H.; Niki, S.; Fujiwara, H. Quantitative determination of optical and recombination losses in thin-film photovoltaic devices based on external quantum efficiency analysis. *J. Appl. Phys.* **2016**, *120*, 064505. [CrossRef]
20. Matin, M.A.; Tomal, M.U.; Robin, A.M.; Amin, N. Numerical Analysis of Novel Back Surface Field for High Efficiency Ultrathin CdTe Solar Cells. *Int. J. Photoenergy* **2013**, *2013*, 1–8. [CrossRef]
21. Lin, Q.; Su, Y.; Zhang, M.-J.; Yang, X.; Yuan, S.; Hu, J.; Lin, Y.; Liang, J.; Pan, F. A novel p-type and metallic dual-functional Cu–Al2O3 ultra-thin layer as the back electrode enabling high performance of thin film solar cells. *Chem. Commun.* **2016**, *52*, 10708–10711. [CrossRef]
22. Zhao, F.; Chen, X.; Yi, Z.; Qin, F.; Tang, Y.; Yao, W.; Zhou, Z.; Yi, Y. Study on the solar energy absorption of hybrid solar cells with trapezoid-pyramidal structure based PEDOT:PSS/c-Ge. *Sol. Energy* **2020**, *204*, 635–643. [CrossRef]
23. Janik, E.; Triboulet, R. Ohmic contacts to p-type cadmium telluride and cadmium mercury telluride. *J. Phys. D: Appl. Phys.* **1983**, *16*, 2333–2340. [CrossRef]
24. Ye, M.; Zhang, D.; Yap, Y.K. Recent Advances in Electronic and Optoelectronic Devices Based on Two-Dimensional Transition Metal Dichalcogenides. *Electronics* **2017**, *6*, 43. [CrossRef]
25. Balandin, A.A.; Ghosh, S.; Bao, W.; Calizo, I.; Teweldebrhan, D.; Miao, F.; Lau, C.N. Superior thermal conductivity of single-layer grapheme. *Nano Lett.* **2008**, *8*, 902–907. [CrossRef] [PubMed]
26. Ganz, E.; Ganz, A.B.; Yang, L.-M.; Dornfeld, M. The initial stages of melting of graphene between 4000 K and 6000 K. *Phys. Chem. Chem. Phys.* **2017**, *19*, 3756–3762. [CrossRef]
27. Gautam, M.; Jayatissa, A.H. Gas sensing properties of graphene synthesized by chemical vapor deposition. *Mater. Sci. Eng. C* **2011**, *31*, 1405–1411. [CrossRef]

28. Gautam, M.; Jayatissa, A.H. Ammonia gas sensing behavior of graphene surface decorated with gold nanoparticles. *Solid-State Electron.* **2012**, *78*, 159–165. [CrossRef]
29. Park, D.-W.; Schendel, A.A.; Mikael, S.; Brodnick, S.K.; Richner, T.J.; Ness, J.P.; Hayat, M.R.; Atry, F.; Frye, S.T.; Pashaie, R.; et al. Graphene-based carbon-layered electrode array technology for neural imaging and optogenetic applications. *Nat. Commun.* **2014**, *5*, 5258. [CrossRef]
30. Yu, T.; Wang, F.; Xu, Y.; Ma, L.; Pi, X.; Yang, D. Graphene Coupled with Silicon Quantum Dots for High-Performance Bulk-Silicon-Based Schottky-Junction Photodetectors. *Adv. Mater.* **2016**, *28*, 4912–4919. [CrossRef] [PubMed]
31. Narayanan, R.; Yamada, H.; Karakaya, M.; Podila, R.; Rao, A.M.; Bandaru, P.R. Modulation of the electrostatic and quantum capacitances of few layered graphenes through plasma processing. *Nano Lett.* **2015**, *15*, 3067–3072. [CrossRef]
32. De Arco, L.G.; Zhang, Y.; Schlenker, C.W.; Ryu, K.; Thompson, M.; Zhou, C. Continuous, Highly Flexible, and Transparent Graphene Films by Chemical Vapor Deposition for Organic Photovoltaics. *ACS Nano* **2010**, *4*, 2865–2873. [CrossRef]
33. Czerniak-Reczulska, M.; Niedzielska, A.; Jędrzejczak, A. Graphene as a Material for Solar Cells Applications. *Adv. Mater. Sci.* **2015**, *15*, 67–81. [CrossRef]
34. Yi, Z.; Li, J.; Lin, J.; Qin, F.; Chen, X.; Yao, W.; Liu, Z.; Cheng, S.; Wu, P.; Li, H. Broadband polarization-insensitive and wide-angle solar energy absorber based on tungsten ring-disc array. *Nanoscale* **2020**, *12*, 23077–23083. [CrossRef] [PubMed]
35. Ciuk, T.; Kaszub, W.; Kosciewicz, K.; Dobrowolski, A.; Jagiello, J.; Chamryga, A.; Gaca, J.; Wojcik, M.; Czolak, D.; Stanczyk, B.; et al. Highly-doped p-type few-layer graphene on UID off-axis homoepitaxial 4H–SiC. *Curr. Appl. Phys.* **2021**, *27*, 17–24. [CrossRef]
36. Zhou, D.; Zhou, T.; Tian, Y.; Zhu, X.; Tu, Y. Perovskite-Based Solar Cells: Materials, Methods, and Future Perspectives. *J. NanoMater.* **2018**, *2018*, 1–15. [CrossRef]
37. Fonash, S.J. *Solar Cell Device Physics*, 2nd ed.; Academic Press: Cambridge, MA, USA, 2010.
38. Shah, D.K.; Kc, D.; Akhtar, M.S.; Kim, C.Y.; Yang, O.-B. Vertically Arranged Zinc Oxide Nanorods as Antireflection Layer for Crystalline Silicon Solar Cell: A Simulation Study of Photovoltaic Properties. *Appl. Sci.* **2020**, *10*, 6062. [CrossRef]
39. Belarbi, M.; Benyoucef, A.; Benyoucef, B. Simulation of the Solar Cells with PC1D, Application to Cells Based on Silicon. *AEIJ* **2014**, *1*, 3–13.
40. Devendra, K.C.; Wagle, R.; Gaib, R.; Shrivastava, A.; Mishra, L.N. Modelling and simulation of AlGaAs/GaAs solar cell. *Am. J. Eng. Res.* **2020**, *9*, 218–223.
41. Ameen, S.; Akhtar, M.S.; Shin, H.S. Highly dense ZnO nanowhiskers for the low level detection of p-hydroquinone. *Mater. Lett.* **2015**, *155*, 82–86. [CrossRef]
42. Weiss, T.P.; Bissig, B.; Feurer, T.; Carron, R.; Buecheler, S.; Tiwari, A.N. Bulk and surface recombination properties in thin film semiconductors with different surface treatments from time-resolved photoluminescence measurements. *Sci. Rep.* **2019**, *9*, 1–13. [CrossRef]
43. Devendra, K.C.; Wagle, R.; Gaib, R.; Shrivastava, A.; Mishra, L.N. InGaP Window Layer for Gallium Arsenide (GaAs) based Solar Cell Using PC1D Simulation. *JARDCS* **2020**, *12*. [CrossRef]
44. Tinedert, I.E.; Pezzimenti, F.; Megherbi, M.; Saadoune, A. Design and simulation of a high efficiency CdS/CdTe solar cell. *Optik* **2020**, *208*, 164112. [CrossRef]
45. Marjani, S.; Khosroabadi, S.; Sabaghi, M. A High Efficiency Ultrathin CdTe Solar Cell for Nano-Area Applications. *Opt. Photonics J.* **2016**, *06*, 15–23. [CrossRef]
46. Fathil, M.; Arshad, M.M.; Hashim, U.; Ruslinda, A.R.; Ayub, R.M.; Azman, A.; Nurfaiz, M.; Kamarudin, M.; Aminuddin, M.; Munir, A. The impact of minority carrier lifetime and carrier concentration on the efficiency of CIGS solar cell. In Proceedings of the IEEE International Conference on Semiconductor Electronics (IEEE-ICSE2014), Kuala Lumpur, Malaysia, 27–29 August 2014; pp. 24–27.
47. Kc, D.; Shah, D.K.; Alanazi, A.M.; Akhtar, M.S. Impact of Different Antireflection Layers on Cadmium Telluride (CdTe) Solar Cells: A PC1D Simulation Study. *J. Electron. Mater.* **2021**, *50*, 2199–2205. [CrossRef]
48. Singh, G.; Kumar, R. Simulation of perovskite solar cell with graphene as hole transporting material. *AIP Conf. Proc.* **2019**, *2115*, 030548.
49. Shah, D.K.; Kc, D.; Muddassir, M.; Akhtar, M.S.; Kim, C.Y.; Yang, O.-B. A simulation approach for investigating the performances of cadmium telluride solar cells using doping concentrations, carrier lifetimes, thickness of layers, and band gaps. *Sol. Energy* **2021**, *216*, 259–265. [CrossRef]
50. Larousu, E.; El-Zohry, A.M.; Yin, J.; Zhumekenov, A.A.; Yang, C.; Alhabshi, E.; Gereige, I.; AlSaggaf, A.; Malko, A.V.; Bakr, O.M. Ultralong Radiative States in Hybrid Perovskite Crystals: Compositions for Submillimeter Diffusion Lengths. *J. Phys. Chem. Lett.* **2017**, *8*, 4386–4390. [CrossRef] [PubMed]
51. Zhao, H.; Farah, A.; Morel, D.; Ferekides, C. The effect of impurities on the doping and VOC of CdTe/CdS thin film solar cells. *Thin Solid Films* **2009**, *517*, 2365–2369. [CrossRef]
52. Desnica, U.V. Doping Limits in II-Vl Compounds—Challenges, Problems and Solutions. *Prog. Cryst. Growth Charact. Mater.* **1998**, *36*, 291–357. [CrossRef]
53. Zhao, Y.; Liang, C.; Sun, M.; Liu, Q.; Zhang, F.; Li, D.; He, Z. Effect of doping on the short-circuit current and open-circuit voltage of polymer solar cells. *J. Appl. Phys.* **2014**, *116*, 154506. [CrossRef]

54. Bätzner, D.; Wendt, R.; Romeo, A.; Zogg, H.; Tiwari, A. A study of the back contacts on CdTe/CdS solar cells. *Thin Solid Films* **2000**, *361–362*, 463–467. [CrossRef]
55. Ning, T.; Isaac, R. Effect of emitter contact on current gain of silicon bipolar devices. In Proceedings of the 1979 International Electron Devices Meeting, Washington, DC, USA, 3–5 December 1979; pp. 2051–2055. [CrossRef]
56. Uprety, P.; Subedi, I.; Junda, M.M.; Collins, R.W.; Podraza, N.J. Photogenerated Carrier Transport Properties in Silicon Photovoltaics. *Sci. Rep.* **2019**, *9*, 1–12. [CrossRef]
57. Available online: http://www.pveducation.org/pvcdrom/pn-junction/band-gap (accessed on 2 April 2021).
58. Zhao, P.Q.; Liu, L.Z.; Xue, H.; Wu, X.L.; Shen, J.C.; Chu, P.K. Resonant Raman scattering from CdS nanocrystals enhanced by interstitial Mn. *Appl. Phys. Lett.* **2013**, *102*, 061910. [CrossRef]
59. Ali, A.M.; Rahman, K.; Ali, L.M.; Akhtaruzzaman, M.; Sopian, K.; Radiman, S.; Amin, N. A computational study on the energy bandgap engineering in performance enhancement of CdTe thin film solar cells. *Results Phys.* **2017**, *7*, 1066–1072. [CrossRef]
60. Jin, Y.; Zheng, Y.; Podkolzin, S.G.; Lee, W. Band gap of reduced graphene oxide tuned by controlling functional groups. *J. Mater. Chem. C* **2020**, *8*, 4885–4894. [CrossRef]
61. Shi, Z.; Jayatissa, A.H. The Impact of Graphene on the Fabrication of Thin Film Solar Cells: Current Status and Future Prospects. *Materials* **2017**, *11*, 36. [CrossRef]
62. Romeo, A.; Khrypunov, G.; Galassini, S.; Zogg, H.; Tiwari, A. Bifacial configurations for CdTe solar cells. *Sol. Energy Mater. Sol. Cells* **2007**, *91*, 1388–1391. [CrossRef]
63. Aldosari, M.; Sohrabpoor, H.; Gorji, N.E. Optical modeling of graphene contacted CdTe solar cells. *Superlattices Microstruct.* **2016**, *92*, 242–248. [CrossRef]